Supplementary Material for

Phonon Scattering Mechanism in Thermoelectric Materials Revised via Resonant X-ray Dynamical Diffraction

Adriana Valério, Rafaela F. S. Penacchio, Maurício B. Estradiote, Marli R. Cantarino, Fernando A. Garcia, and Sérgio L. Morelhão, Institute of Physics, University of São Paulo, São Paulo, SP, Brazil

Niamh Rafter and Stefan W. Kycia, Department of Physics, University of Guelph, Guelph, Ontario N1G 1W2, Canada

Guilherme A. Calligaris, Brazilian Synchrotron Light Laboratory - LNLS/CNPEM, Campinas, SP, Brazil

Cláudio M. R. Remédios, Instituto de Ciências Exatas e Naturais, Universidade Federal do Pará, Belém, PA, Brazil

Address all correspondence to Sérgio L. Morelhão at morelhao@if.usp.br

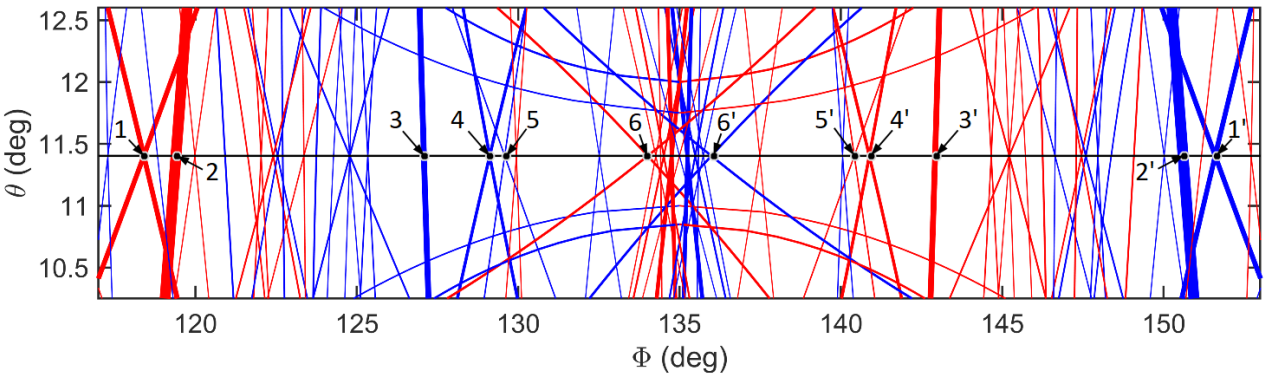

#	h,k,l	Φ (deg)	Ψ (deg)
1	-1,3,4/-1,3,-2	118.404	-175.7
2	0,3,1	119.400	-179.6
3	-3,-4,1	127.081	-176.5
4	-7,-3,4/-7,-3,-2	129.120	-172.5
5	-1,-2,3/-1,-2,-1	129.584	-162.8
6	-2,1,5/-2,1,-3	134.013	-170.1

#	h,k,l	Φ (deg)	Ψ (deg)
6'	-2,-1,5/-2,-1,-3	135.987	-170.1
5'	-1,2,3/-1,2,-1	140.416	-162.8
4'	-7,3,4/-7,3,-2	140.880	-172.5
3'	-3,4,1	142.919	-176.5
2'	0,-3,1	150.600	-179.6
1'	-1,-3,4/-1,-3,-2	151.596	-175.7

Fig. S1: (Top panel) BC lines for indexing the azimuthal scan of the 002 $CeFe_4P_{12}$ reflection obtained with characteristic radiation of 8048 eV [Fig. 1(d), main text]. BC line of reflection 002 (horizontal solid-black line) at the Bragg angle θ = 11.403°. (Bottom panel) hkl indexes of a few BC lines, Φ positions of intersection points corresponding to the observed peaks in the experimental azimuthal scan (a = 7.7920 Å), and calculated phase triplets Ψ for a model structure with isotropic RMS atomic displacement of 10 pm set to all elements.

S1. Graphical indexing of azimuthal scans

The reliability in correlating asymmetric intensity profiles and phase triplet values can be compromised by overlapping of peaks with different phases. The most straightforward approach to index and select suitable n-beam diffraction peaks for extracting phase information is the 2D representation of Bragg cones (BCs) as a function of the instrumental angles θ and Φ.[1,2] It is shown in Fig. S1 where each line stands for the diffraction condition of one reflection of the crystal. As simultaneous diffractions take place at cone intersections, the azimuthal scan technique is able to detect intensity modulations of the reference reflection at Φ positions where its BC line (parallel to the Φ-axis) is crossed by other BC lines. Numbered crossing points in Fig. S1 (top panel) stand for the

numbered n-beam diffraction peaks in the experimental scan presented in the main text, Fig. 1(d). All peaks are either three-beam (single BC line) or systematic four-beam diffractions (two BC lines forming an X). In a three-beam diffraction there is only one secondary wave interfering with the reference wave, while in a systematic four-beam diffraction two secondary waves of identical phases are produced. Therefore, both three- and four-beam diffractions can provide useful phase information.

Peak asymmetries are determined by the phase triplet values Ψ, and by the diffraction geometry of the secondary reflection where the incident X-ray beam is entering or exiting the aperture of the Bragg cone.[3-12] These two geometries are indicated by blue (entering) or red (exiting) BC lines in Fig. S1. It implies that when taking note of the peak asymmetry, lower/higher (L/H) or higher/lower (H/L) shoulders, it is also necessary to take note of the diffraction geometry that is given by the color of the lines in this graphical indexing method used here. For instance, peaks 2 (red) and 2' (blue) are equivalent in terms of phase information as they have exactly the same Ψ values although appearing with opposite asymmetries in the azimuthal scan [Fig. 1(d), main text].

The entering $\Phi_{\mathrm{blue}} = \alpha_{hk} - \beta_{hkl}$ and exiting $\Phi_{\mathrm{red}} = \alpha_{hk} + \beta_{hkl}$ positions of the peaks in the azimuthal scans of reflection 002 can also be calculated analytically by taking $\beta_{hkl} = \cos^{-1}\left(\frac{h^2+k^2+l(l-2)}{2\sqrt{(a/\lambda)^2-1}\sqrt{h^2+k^2}}\right)$ and $\alpha_{hk} = \tan^{-1}\left(\frac{k-h}{h+k}\right)$ were hkl are the reflection indexes of the secondary reflection.[13] For instance, reflections 101, 011, $\bar{1}01$, and $0\bar{1}1$ all have $\beta_{hkl} = 90°$ and $\alpha_{hk} = -45°$, $45°$, $135°$, and $-135°$, respectively; note that the arctan function must be calculated with respect to the four trigonometric quadrants. The experimental peaks at mirroring positions such as $\Phi = 45°$ $(101/\bar{1}01)$ and $\Phi = 135°$ $(011/0\bar{1}1)$ have simultaneous contributions of two of these reflections, one at the entering and the other at the exiting geometry, whose opposite asymmetries cancel each other to provide symmetric peaks regardless the used X-ray energy. This coincidental overlapping is broken only when the cubic lattice undergoes tetragonal distortion, as observed in epitaxial films.[14]

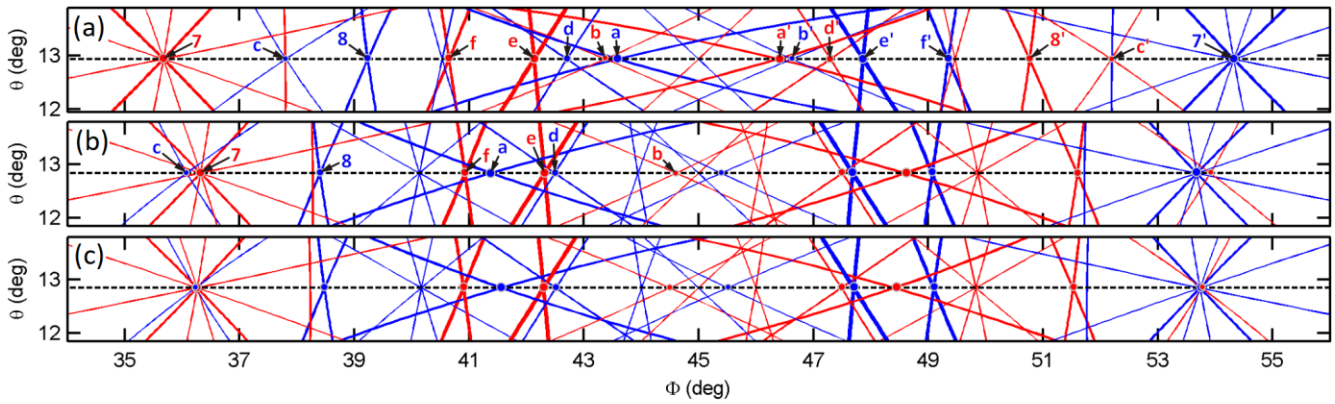

		7105.8 eV (a = 7.7920 Å)		7161.2 eV (a = 7.7920 Å)		(a = 7.7862 Å)
label	h,k,l	Φ (deg)	Ψ_1 (deg)	Φ (deg)	Ψ_2 (deg)	Φ (deg)
	4,4,4/4,4,-2		1.4		116.0	
7	1,1,4/1,1,-2	35.676	29.4	36.320	149.7	36.259
	5,5,2/5,5,0		26.8		147.2	
c	-1,8,3/-1,8,-1	37.809	27.6	36.083	148.0	36.240
8	-3,7,2/-3,7,0	39.233	10.7	38.401	131.4	38.479
f	4,2,2/4,2,0	40.650	178.6	40.929	-53.3	40.902
e	3,1,2/3,1,0	42.133	5.1	42.315	125.9	42.297
d	-2,1,3/-2,1,-1	42.703	13.9	42.493	134.5	42.513
b	2,5,5/2,5,-3	43.373	24.3	44.606	144.8	44.492
a	-1,6,5/-1,6,-3	43.602	10.9	41.392	131.6	41.587

Fig. S2: (Top panel) BC lines for indexing the azimuthal scans of the 002 $CeFe_4P_{12}$ reflection obtained with synchrotron X-rays of (a) 7105.8 eV and (b,c) 7161.2 eV [Fig. 3(a-c), main text]. BC line of reflection 002 (dashed-black line) at the Bragg angle θ = 12.940°, 12.838°, and 12.948°, respectively. (Bottom panel) hkl indexes of a few BC lines, Φ positions of intersection points, and calculated phase triplets $\Psi_{1,2}$ for each energy in a model structure with isotropic RMS atomic displacement of 10 pm set to all elements.

In terms of constructing asymmetry matching diagrams (AMDs) to validate model structures, taking into account equivalent peaks is unnecessary, as well as performing phase calculation for both secondary waves of systematic four-beam diffractions. Crystal symmetry and chosen rotation axis determines the angular range of azimuthal scans containing non-redundant phase information. For rotation axis with 4-fold symmetry, the available phase information is repeated every 45° of rotation. In the $CeFe_4P_{12}$ structure, only peak positions obey the 4-fold symmetry of the cubic unit cell [001] crystallographic axis. As hkl and khl reflections have in general different structure factors, the [001] axis is in fact a 2-fold symmetry axis, demanding Φ-scans of at least 90° to collect the complete set of

phase information experimentally accessible when using 002 as the reference reflection. See Table SI for the experimental peaks used to generate the AMD for X-rays of 8048 eV in Fig. 4(b).

S2. Resonant phase shift

Graphical indexing of azimuthal scans obtained with synchrotron X-rays of 7105.8 eV and 7161.2 eV are given in Fig. S2 (top panel). Crossing points of BC lines are labeled with number and letters to easily visualize how the peak positions change from one energy to the other. Inversion of peak asymmetry occurs when $\cos(\Psi_1)\cos(\Psi_2) < 1$ where Ψ_1 and Ψ_2 are phase triplet values for each energy, as detailed in the bottom panel of Fig. S2. The small shifts in peak positions caused by reduction in temperature can be seen by comparing BC lines in Fig. S2(b,c). Peaks corresponding to crossing points with more than two BC lines, such as points 7 and 7' in Fig. S2, were not taken into account for asymmetry matching analysis because the multiple secondary waves generated at such overlapping of lines have different phases. Predict the exact energy in which such 8-beam diffraction undergoes an inversion of peak asymmetry demand a more sophisticated analysis than the second-order approximation employed here.[4,6,9,10] On the other hand, the angular separation between these peaks were used to calibrate the X-ray energies of all synchrotron data at room temperature, as well as the lattice parameter a = 7.7862 Å at a lower temperature near 150 K.[14-17]

Resonant diffraction is known to change phase triplet values and n-beam peak asymmetries.[6,10] However, the giant and abrupt phase shift of reflection 002 is a new fact that has its roots on the interleaved stacking of Ce and Fe planes along the [001] type direction. The X-ray scattering from the atomic planes of Ce and P nearly cancel the scattering from the atomic planes of Fe, as shown in Fig. S3(a,b). Atomic scattering factors were calculated for Ce^{3+}, Fe^{2+}, and P^{1-} ions by using MatLab codes asfQ.m, while f' and f'' for all elements by codes fpfpp.m.[18]

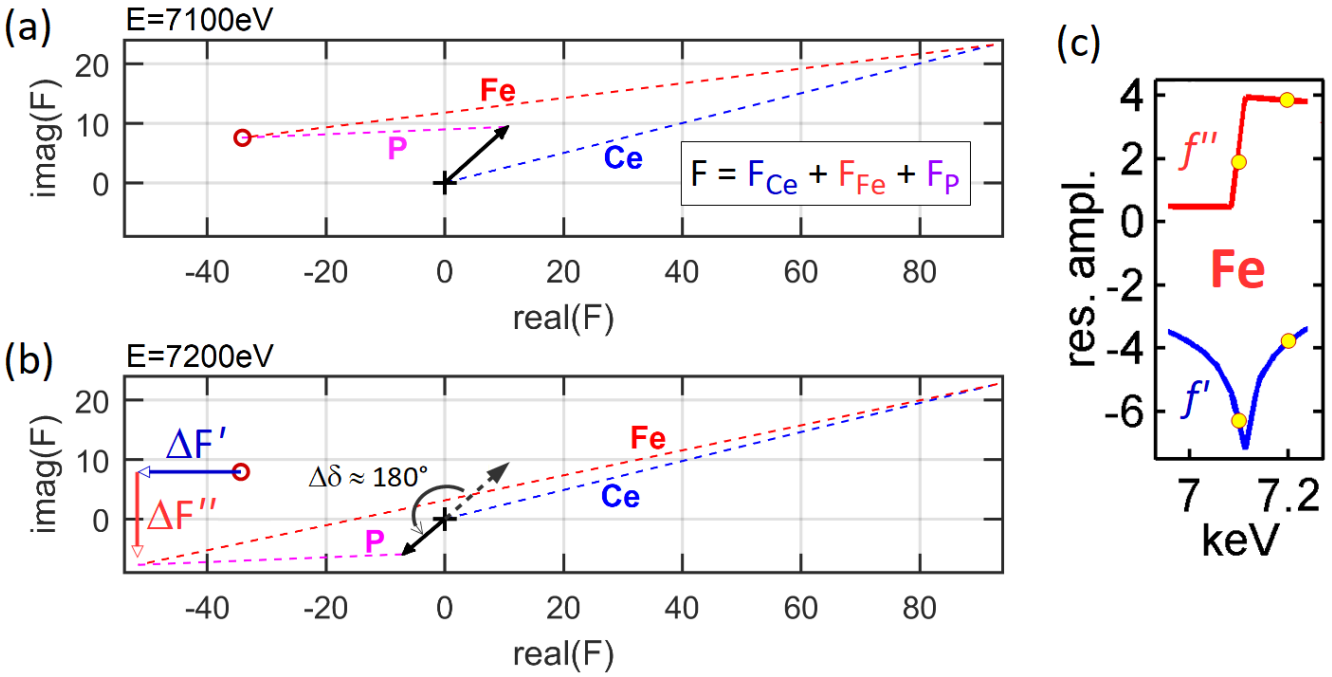

Fig. S3: (a,b) Argand diagrams for structure factor $F = F_{Ce} + F_{Fe} + F_P$ of the 002 reflection of $CeFe_4P_{12}$ crystal. X-ray energies of (a) 7100 eV and (b) 7200 eV. The individual contributions of each element are shown by dashed lines. (c) Resonant atomic scattering amplitudes f' and f'' of Fe around its absorption *K* edge, values for 7.1 keV and 7.2 keV are indicated (yellow circles). Changes $\Delta f'$ and $\Delta f''$ in these resonant amplitudes produce changes $\Delta F' \approx -8\Delta f'$ and $\Delta F'' \approx -8\Delta f''$ in the real and imaginary terms of F, resulting in a phase shift $\Delta\delta$ of nearly 180°.

S3. Experimental peak asymmetries

The experimental peaks of n-beam diffraction used to validate structural models via asymmetry matching diagrams are listed in Fig. S4. Three-beam diffractions have the last index $l = 1$. All others are systematic four-beam diffractions where only one secondary reflection is listed for each case. For instance, "215 H b" in Fig. S4(a) denotes the four-beam diffraction $215/21\bar{3}$ with asymmetry of higher/lower shoulder in entering (blue BC line) diffraction geometry at the azimuth Φ = 316.0°. The phase triplets Ψ come from $W = F_{hkl}F_{002-hkl}/F_{002} = |W|\exp(i\Psi)$.[2]

(a)

h	k	l	asy.	diff.	Φ (deg)	h	k	l	asy.	diff.	Φ (deg)
2	4	0	L	b	315.2	2	-1	3	L	r	357.3
4	4	4	H	b	315.5	4	-1	3	L	r	1.7
2	1	5	H	b	316.0	-1	2	3	H	b	2.7
3	5	0	H	b	320.1	4	4	6	H	r	3.3
1	-2	3	L	r	320.4	1	6	5	H	b	5.1
7	-3	4	L	r	320.9	-1	6	3	H	b	6.0
3	-4	1	L	r	322.9	2	1	5	L	r	7.1
0	2	0	L	b	326.6	7	3	4	L	r	7.3
5	-3	4	L	r	327.5	4	1	5	L	r	7.5
2	4	4	H	b	327.6	2	0	4	H	r	7.8
9	4	1	H	b	328.4	4	0	4	H	r	7.8
2	-3	1	L	r	329.1	3	-1	2	L	r	8.0
0	3	1	H	b	330.6	-1	1	0	H	b	8.2
1	3	4	H	b	331.6	-1	3	4	H	b	8.5
9	-1	0	L	r	332.7	2	7	5	H	b	9.4
6	-3	1	L	r	337.0	0	9	1	H	b	18.7
7	0	5	L	r	337.8	-2	4	4	H	b	20.7
4	5	5	H	b	338.2	-3	4	1	H	b	20.8
4	-2	4	L	r	339.3	1	0	3	L	r	21.2
4	-1	5	L	r	339.5	-1	6	5	H	b	24.0
3	7	0	H	b	342.0	-3	7	0	H	b	28.4
0	5	1	H	b	344.0	-2	1	1	H	b	28.8
9	1	0	L	r	345.4	4	1	3	L	r	29.8
9	4	1	L	r	349.5	6	3	1	L	r	30.2
5	0	5	L	r	351.2	-3	2	1	H	b	30.9
4	-2	0	H	r	351.6	4	2	4	L	r	32.4
3	-2	1	L	r	351.7	2	0	0	H	r	33.4
1	-1	0	L	r	351.8	-2	1	3	H	b	39.6
-1	2	1	H	b	352.0	-2	7	5	H	b	41.3
0	2	4	L	b	352.2	-4	7	3	H	b	43.0
0	4	4	L	b	352.2	1	2	5	L	r	44.0
1	2	5	H	b	352.9	4	4	4	L	r	44.5
7	0	3	L	r	356.5	4	2	0	H	r	44.8
4	4	6	L	b	356.7	3	1	0	L	r	44.8

(b)

h	k	l	asy.	diff.	Φ (deg)	h	k	l	asy.	diff.	Φ (deg)
4	-2	4	H	r	332.4	6	6	2	H	r	12.9
7	3	4	L	b	332.8	-1	6	3	L	b	13.5
2	4	4	L	b	334.4	-1	3	4	L	b	14.3
1	4	3	L	b	334.8	6	5	3	H	r	14.5
6	5	3	L	b	335.1	3	2	5	H	r	15.5
6	1	5	H	r	335.3	3	7	4	L	b	16.4
2	5	3	L	b	336.2	1	0	3	H	r	17.6
1	3	4	L	b	337.4	5	7	2	H	r	18.3
5	5	4	L	b	340.4	-2	3	3	L	b	19.3
3	-2	3	H	r	340.7	5	5	4	H	r	19.6
7	1	4	H	r	342.7	5	3	4	H	r	20.1
7	3	4	H	r	343.6	5	1	2	H	r	20.5
2	3	5	L	b	344.5	0	3	5	L	b	21.8
3	4	5	L	b	344.9	3	1	4	H	r	22.6
5	6	3	L	b	345.5	6	5	1	H	r	22.9
3	-1	4	H	r	345.7	1	8	3	L	b	23.6
7	0	3	H	r	346.4	5	2	3	H	r	23.8
6	6	2	L	b	347.1	1	6	5	L	b	24.7
4	-2	2	L	r	347.5	5	6	3	H	r	24.9
8	2	2	H	r	347.7	4	1	3	H	r	25.2
3	-2	1	H	r	348.8	-3	4	1	L	b	25.3
0	5	1	L	b	348.5	4	2	4	H	r	25.6
8	3	1	H	r	350.1	3	7	4	H	r	27.2
1	-1	2	H	r	350.6	-2	4	4	L	b	27.6
3	7	2	L	b	352.8	4	7	3	H	r	29.6
-1	2	1	L	b	353.4	-2	1	1	L	b	30.3
1	5	4	L	b	353.7	3	4	5	H	r	31.3
2	-1	3	H	r	354.2	5	4	3	H	r	31.5
1	6	3	L	b	354.6	2	0	2	H	r	31.7
-1	3	2	L	b	354.7	-3	4	3	L	b	31.9
4	1	5	H	r	356.0	-1	4	5	L	b	32.1
5	2	5	H	r	357.0	4	1	1	H	r	32.6
4	-1	3	H	r	357.1	-2	7	3	L	b	33.0
5	-1	2	H	r	357.8	-3	2	1	L	b	33.8
5	7	2	L	b	0.7	4	4	4	H	r	35.7
4	7	3	L	b	0.9	-1	8	3	L	b	37.8
2	7	3	L	b	1.1	2	3	5	H	r	38.2
-1	4	3	L	b	2.9	3	8	1	H	r	39.0
2	5	5	L	b	3.0	-3	7	2	L	b	39.2
1	4	5	L	b	4.0	-2	8	2	L	b	40.4
5	0	3	H	r	5.0	-4	4	2	L	b	40.5
3	-1	2	H	r	5.3	4	2	2	L	r	40.7
-1	2	3	L	b	5.8	-3	2	3	L	b	42.0
5	1	4	H	r	6.3	3	1	2	H	r	42.1
2	-1	1	H	r	6.6	-2	1	3	L	b	42.7
-1	1	2	L	b	9.4	2	5	5	H	r	43.4
3	8	1	L	b	9.9	-1	6	5	L	b	43.6
-2	3	1	L	b	11.2	4	5	3	H	r	44.2

(c)

h	k	l	asy.	diff.	Φ (deg)	h	k	l	asy.	diff.	Φ (deg)
5	-4	3	L	r	314.6	5	7	2	H	b	358.9
5	4	3	H	b	315.4	7	2	3	L	r	359.4
1	3	2	H	b	317.7	4	7	3	H	b	359.8
2	-3	3	L	r	318.2	2	7	3	H	b	0.6
2	4	2	L	b	319.2	7	5	2	L	r	1.1
8	3	1	H	b	319.9	-1	4	3	H	b	2.7
3	2	5	H	b	321.2	1	4	5	H	b	3.4
7	-3	2	L	r	321.3	3	-1	2	L	r	5.4
8	-1	3	L	r	323.4	5	1	4	L	r	6.7
6	-3	3	L	r	323.6	-2	4	2	L	b	12.3
4	4	4	H	b	323.9	3	7	4	H	b	13.8
2	-3	1	L	r	326.3	-1	3	4	H	b	14.0
7	-2	3	L	r	327.5	6	5	3	L	r	15.4
4	5	3	H	b	328.1	3	2	5	L	r	16.1
4	-1	5	L	r	328.5	6	3	3	L	r	16.7
7	3	4	H	b	330.2	1	0	3	L	r	17.8
0	3	1	H	b	332.7	-2	3	3	H	b	19.2
2	4	4	H	b	334.1	5	7	2	L	r	20.1
6	5	3	H	b	334.2	1	8	3	H	b	22.4
1	4	3	H	b	334.6	3	1	4	L	r	22.9
1	3	4	H	b	337.1	2	5	7	H	b	23.2
8	1	3	L	r	337.6	-3	4	1	H	b	25.1
3	5	4	H	b	339.4	5	6	3	L	r	25.8
7	5	2	H	b	339.9	4	2	4	L	r	25.9
3	-2	3	L	r	340.8	-2	4	4	H	b	27.2
7	1	4	L	r	343.5	3	7	4	L	r	29.8
2	3	5	H	b	343.9	4	7	3	L	r	30.7
5	-1	4	L	r	344.1	-1	4	5	H	b	31.5
3	4	5	H	b	344.2	-3	4	3	H	b	31.7
5	6	3	H	b	344.6	3	4	5	L	r	32.1
3	-1	4	L	r	346.0	-2	7	3	H	b	32.5
7	3	4	L	r	346.2	-3	2	1	H	b	33.7
4	-2	2	H	r	347.7	4	4	4	L	r	36.1
6	0	4	H	r	348.1	-1	8	3	H	b	36.6
0	5	1	H	b	348.3	-3	7	2	H	b	38.7
3	-2	1	L	r	349.0	2	3	5	L	r	38.8
8	3	1	L	r	351.2	4	2	2	H	r	40.8
5	4	5	H	b	351.5	-3	2	3	H	b	41.8
3	7	2	H	b	352.3	-1	6	5	H	b	42.1
-1	3	2	H	b	354.6	3	1	2	L	r	42.3
0	5	3	H	b	354.8	4	5	3	L	r	44.6
5	4	5	L	r	355.8	-4	5	3	H	b	45.4
4	1	5	L	r	356.6						

Fig. S4: List of hkl secondary reflections, observed peak asymmetries (asy.), diffraction geometries (diff.), and Φ positions for (a) Cu$K\alpha_1$ radiation (8048 eV),[19,20] and synchrotron X-rays of energies (b) 7105.8 eV and (c) 7142.3 eV. L or H letters stand for peaks with lower/higher or higher/lower shoulders. Diffraction geometries of entering or exiting the Bragg cone are represented by letter b (blue BC lines) or r (red BC lines), respectively.

References

1. J. Z. Domagała, S. L. Morelhão, M. Sarzyński, M. Maździarz, P. Dłużewski, and M. Leszczyński: Hybrid reciprocal lattice: application to layer stress determination in GaAlN/GaN(0001) systems with patterned substrates. J. Appl. Cryst. 49, 798 (2016).

2. S. L. Morelhão, C. M. R. Remédios, G. A. Calligaris, and G. Nisbet. X-ray dynamical diffraction in amino acid crystals: a step towards improving structural resolution of biological molecules via physical phase measurements. J. Appl. Cryst. 50, 689 (2017).

3. S. L. Morelhão and L. H. Avanci: Strength tuning of multiple waves in crystals. Acta Cryst. A 57, 192 (2001).

4. S. L. Morelhão and S. Kycia: Enhanced X-ray phase determination by three-beam diffraction. Phys.

Rev. Lett. 89, 015501 (2002).

5. S. L. Morelhão: An X-ray diffractometer for accurate structural invariant phase determination. J. Synchrotron Radiat. 10, 236 (2003).

6. S. L. Morelhão: Accurate triplet phase determination in non-perfect crystals–a general phasing procedure. Acta Cryst. A 59, 470 (2003).

7. S. L. Morelhão, L. H. Avanci, and S. Kycia: Study of crystalline structures via physical determination of triplet phase invariants. Nucl. Instrum. Meth. B 238, 175 (2005).

8. S. L. Morelhão, L. H. Avanci, and S. Kycia: Automatic X-ray crystallographic phasing at LNLS. Nucl. Instrum. Meth. B 238, 180 (2005).

9. S. L. Morelhão, L. H. Avanci, and S. Kycia: Energy conservation in approximated solutions of multi-beam scattering problems. Nucl. Instrum. Meth. B 239, 245 (2005).

10. S. L. Morelhão, C. M. R. Remédios, R. O. Freitas, and A. O. dos Santos: X-ray phase measurements as a probe of small structural changes in doped nonlinear optical crystals. J. Appl. Cryst. 44, 93 (2011).

11. Z. G. Amirkhanyan, C. M. R. Remédios, Y. P. Mascarenhas, and S. L. Morelhão: Analyzing structure factor phases in pure and doped single crystals by synchrotron X-ray Renninger scanning. J. Appl. Cryst. 47, 160 (2014).

12. S. L. Morelhão, Z. G. Amirkhanyan, and C. M. R. Remédios: Absolute refinement of crystal structures by X-ray phase measurements. Acta Cryst. A 71, 291 (2015).

13. B. J. Isherwood and C. A. Wallace: The geometry of X-ray multiple diffraction in crystals. Acta Cryst. A27, 119 (1971).

14. A. S. de Menezes, A. O. dos Santos, J. M. A. Almeida, J. R. R. Bortoleto, M. A. Cotta, S. L. Morelhão, and L. P. Cardoso: Direct observation of tetragonal distortion in epitaxial structures through secondary peak split in a synchrotron radiation Renninger scan. Cryst. Growth Des. 10, 3426 (2010).

15. L. H. Avanci, M. A. Hayashi, L. P. Cardoso, S. L. Morelhão, F. Riesz, K. Rakennus, and T. Hakkarainen: Mapping of Bragg-surface diffraction of InP/GaAs(100) structure. J. Cryst. Growth 188, 220 (1998).

16. R. O. Freitas, S. L. Morelhão, L. H. Avanci, and A. A. Quivy: Strain field of InAs QDs on GaAs (001) substrate surface: characterization by synchrotron X-ray Renninger scanning. Microelectr. J. 36, 219 (2005).

17. R. O. Freitas, T. E. Lamas, A. A. Quivy, and S. L. Morelhão: Synchrotron X-ray Renninger scanning for studying strain in InAs/GaAs quantum dot system. Phys. Stat. Sol. A, 204, 2548 (2007).

18. S. L. Morelhão: Computer Simulation Tools for X-ray Analysis, 1st ed. (Springer International

Publishing, Cham, 2016), pp. 213,246.

19. S. L. Morelhão, S. Kycia, S. Netzke, C. I. Fornari, P. H. O. Rappl, and E. Abramof: Hybrid reflections from multiple X-ray scattering in epitaxial bismuth telluride topological insulator films. Appl. Phys. Lett. 112, 101903 (2018).

20. S. L. Morelhão, S. W. Kycia, S. Netzke, C. I. Fornari, P. H. O. Rappl, and E. Abramof: Dynamics of defects in van der Waals epitaxy of bismuth telluride topological insulators. J. Phys. Chem. C 123, 24818 (2019).